RESEARCH CENTER

AMERICAN OPTICAL COMPANY

Southbridge, Massachusetts

TR 599-3

ESR AND OPTICAL ABSORPTION STUDIES OF TRANSITION METAL IONS AND COLOR CENTERS IN GLASS

SEMI ANNUAL TECHNICAL REPORT
NUMBER THREE

1 October 1967 - 31 March 1968

ARPA Order No. 306
Contract No. N00014-67-C-0186

Prepared by

Research Division
American Optical Company
Southbridge, Massachusetts

Project Scientist - Robert J. Landry
Project Scientist - Joseph T. Fournier

July 1968

This research is part of Project DEFENDER under the joint sponsorship of the Advanced Research Projects Agency, Department of Defense and the Office of Naval Research.

ABSTRACT

The Electron Spin Resonance (ESR) spectrum of isolated Cr^{3+} ions at 34.8 kMHz and at 300°K is presented. Analysis of this and the spectrum obtained earlier at 9.49 kMHz serve to verify the initial estimated bounds of $0.3 < |2D| < 1\ cm^{-1}$ for the magnitude of the zero field splitting parameter.[1] In addition, the spectrum at 34.8 kMHz suggests that a direct zero field absorption may be obtained near 0.66 cm^{-1} or 20 kMHz. For exchange coupled Cr^{3+} ions in glass it is shown that as long as the transition energy $h\nu$ dominates the anisotropies, the ESR linewidth is a constant independent of the energy of the microwave photon used. The ESR spectrum of antiferromagnetically exchange coupled Cr^{3+} ions in a phosphate glass at 34.8 kMHz is shown and compared to the spectrum at 9,49 kMHz. Both spectra have a linewidth of about 1000 gauss and demonstrate that the ESR linewidth is independent of the energy of the microwave photon used for $h\nu > Z.F.S.$ The ESR spectra of isolated Cu^{2+} ions in a simple alkali-calcium-silicate glass as a function of the alkali type of modifier ion present are shown. The measured perpendicular magnetic parameters $g_\perp$ and $A_\perp$ for Cu^{2+} in these glasses are included. The variation in the magnetic parameters mentioned above as a function of the type of alkali modifier ion present is small and within the limits of error in measurement. The data indicates no coordination number change and shows that the local environment of the Cu^{2+} ion must be such that the ESR parameters are not very sensitive to an approximate two-fold change in ionic radii of univalent alkali modifier ion present. The effect of ultraviolet (uv) irradiation on the optical absorption spectrum of a laser glass in the wavelength region (200-300) nm is shown. It is demonstrated that the effect of uv irradiation is to cause the glass to become more transparent in the wavelength region (200-280) nm. The "annihilation" spectrum thus observed has a peak at about 220 nm, nearly coincident with the peak of the activation spectrum presented earlier[5], and has a full width at half maximum of about 40 nm. The irradiation induced optical absorption spectrum of this same laser glass over the wavelength region (200-800) nm is shown. An experimental study to determine if the transient color centers which give rise to limit cycle and self Q-switched laser action in glass lasers are related to the room temperature stable color centers is described. The results obtained suggest that the transient color centers are associated with the stable room temperature color centers. A laser system designed to measure the lifetime of the transient color centers is described.

The status of the program for calculation of the electronic structure of tetrahedral hole-trapping centers is reported. Application of an approximate molecular orbital theory involving complete neglect of differential overlap (CNDO) to SiO_4 tetrahedral units with one or more non-bridging oxygen ions is discussed. Means for distinguishing bridging from non-bridging oxygen ions are considered within the framework of the theory. Overlap and one and two-center Coulomb integrals over Slater atomic orbitals have been computed for an SiO_4 tetrahedron using interatomic distances taken from X-ray data in the literature. These integral values and other emperically determined matrix elements required in the molecular orbital calculation are tabulated.

CONTENTS

ILLUSTRATIONS

ESR AND OPTICAL ABSORPTION STUDIES OF TRANSITION METAL IONS AND COLOR CENTERS IN GLASS

Semi-Annual Report Number Three

1. INTRODUCTION

As in the first two semi-annual periods, the work performed on this contract during the third semi-annual period can be classified into studies of transition metal ions in glass, experimental studies of ultraviolet irradiation induced color center defects in glass, and theoretical investigations of color center defects in glass.

The program of study of transition metal ions in glass has been concerned with isolated Cr^{3+} ions, antiferromagnetically exchange coupled Cr^{3+} ion pairs, and isolated Cr^{2+} ions in glass. For isolated Cr^{3+} ions in glass attention was directed to obtaining a better estimate of the magnitude of the zero field splitting parameter $|2D|$ from a correlation of ESR spectra at different frequencies. A more precise estimate for $|2D|$ may obtain from this study as pointed out in the text. For the exchange-coupled Cr^{3+} ion pairs in glass, it was shown earlier[5] that the ESR spectrum for this system will be symmetrical about $g' = 2$, where $g' = h\nu/\beta H$, as long as the transition energy $h\nu$ dominates the anisotropies. In this report, it is shown that the ESR linewidth should also be a constant and independent of the frequency used for the same condition mentioned above. The ESR spectrum at 34.8 kMHz was obtained for this system in order to verify the model used to explain the ESR spectra at 9.49 and 2.05 kMHz. The studies of isolated Cr^{3+} ions and exchange-coupled Cr^{3+} ion pairs are described in Sections 2.1 and 2.2 respectively.

It was shown in the first semi-annual report[4] that Cu^{2+} ions in glass remain well isolated from one another until about 0.5 wt.% CuO, and that below this concentration, they appear to be octahedrally coordinated to oxygen in a crystal field of predominantly axial symmetry.[4] The magnetic parameters measured in ESR experiment are sensitively dependent on the local environment of the paramagnetic ion. Thus, a study of the dependence of the ESR parameters for Cu^{2+} ions on the glass composition can be used as a probe to study the local environment of this ion in glass. To this end a study of the magnetic parameters for Cu^{2+} as a function of the alkali type of modifier ion present in a simple calcium silicate glass was undertaken. The ESR spectra, results and conclusions which obtain from this study are contained in Section 2.3.

The experimental color center defect studies in laser glass included investigations of both permanent and transient color centers, although emphasis was primarily devoted to a study of the transient centers. The room temperature stable effects of ultraviolet irradiation in the wavelength region (200-300) nm was investigated and is described in Section 3.1. In order to properly characterize the transient color centers which give rise to limit cycle and self Q-switched laser action in glass lasers, it is of fundamental importance to determine if they can be associated with the uv induced room temperature stable color centers. The experimental effort to determine if there is a relationship is described in Section 3.2. An experimental laser system to measure the lifetime of the transient color centers is also described in Section 3.2.

The status of the program for calculation of the electronic structure of tetrahedral hole-trapping centers is reported in Section 4.

2. TRANSITION METAL IONS IN GLASS

2.1 Isolated Cr^{3+} Ions in Glass

The zero field splitting of isolated Cr^{3+} ions in a phosphate glass has been estimated to lie in the frequency range 9 through 30 kMHz.[1] A direct measurement of the distribution function in the zero field splitting of isolated Cr^{3+} ions in glass will provide information of fundamental importance concerning the site to site variation in local structure of this ion in glass. Experimentally, it is impractical to search for zero field absorption throughout the entire estimated range above, and since the preliminary search for zero field absorption in the range (18-26) kMHz did not yield a positive result,[5] it becomes important to try to more precisely determine the magnitude of the zero field splitting.

L. L. van Reijan has shown that for an S = 3/2 system, it is sometimes possible to obtain a fairly precise estimate of the magnitude of the zero field splitting from an analysis of the frequency dependence and/or extreme values of the resulting electron spin resonance (ESR) powder spectrum.[2] The analysis involves the use of plots shown in van Reijan's thesis[2] of $h\nu/D$ versus $g\,\beta H/D$, where $h\nu$ is the energy of a microwave photon, where $g\,\beta H = h\nu$ is the usual resonance condition, and where 2D is the zero field splitting parameter.

In Fig. 1 are shown the ESR spectra for isolated Cr^{3+} ions in a phosphate glass showing the frequency dependence of the ESR spectrum for frequencies of 9.49 and 34.8 kMHz.* The base glass

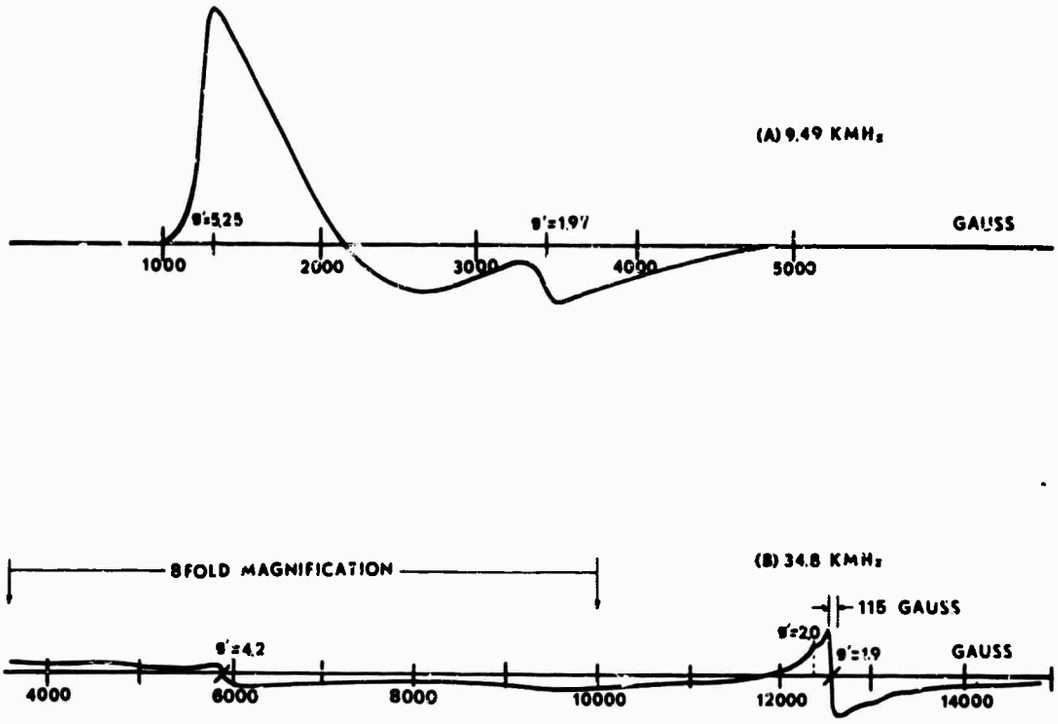

Fig. 1. ESR spectra of isolated Cr^{3+} ions in a phosphate glass at 300°K and at: (a) 9.49 kMHz, and (b) 34.8 kMHz.

studied has the composition of approximately 90 wt.%$Al(PO_3)_3$, 10 wt.% ZnO, and 0.098 wt.% Cr_2O_3. It can be seen from Fig. 1 that the ESR spectra at these two frequencies are quite different. It has been shown before that the ESR spectra at 2.05 and 9.49 kMHz are quite similar to one another, both showing a strong peak in the first derivative curve at about $g' = 5.0$, where $g' = \beta H/h\nu$.[1] The 34.8 kMHz spectrum is quite different from the lower frequency spectra appearing to be fairly isotropic and centered about $g' = 2.0$ with a linewidth of about 115 Gauss and showing a small absorption at $g' = 4.2$.

With the use of van Reijan type plots mentioned above, it is possible to qualitatively account for the spectra observed with $h\nu < 2D$ at 2.05 and 9.49 kMHz and with $h\nu > 2D$ at 34.8 kMHz.

---

*The author gratefully acknowledges Dr. R. Weeks of Oak Ridge National Labs. for obtaining the 34.8 kMHz ESR spectra shown in this report.

Thus, from the 9.49 kMHz spectrum, a lower bound on $|2D|$ of 0.3 cm^{-1} is obtained and from the 34.8 kMHz spectrum, an upper bound on $|2D|$ of 1.0 cm^{-1} is obtained, where 0.3 cm^{-1} and 1.0 cm^{-1} are the approximate energies of the 9.49 and 34.8 kMHz photons, respectively. The upper bound obtained in this manner serves to verify the upper bound previously obtained from a consideration of the optical absorption spectrum for this system.[1] In addition, if the small absorption observed at $g' = 4.2$ in the 34.8 kMHz spectrum truly arises from isolated Cr^{3+} ions, then, use of the plots mentioned above suggests that a zero field splitting absorption may be obtained near 0.66 cm^{-1} or 20 kMHz.

The value of 20 kMHz for $|2D|$ should be taken only as very suggestive of where the zero field absorption might be found since it is not certain that the resonance upon which this estimate is based is due to Cr^{3+}, i.e., the resonance at $g' = 4.2$ may be due to a small amount of Fe^{3+} in the glass. A resonance from Fe^{3+} at $g' = 4.2$ in glass is usually observed at 10 kMHz. However, in the selected few Fe^{3+} containing glasses studied by R. Weeks which show a $g' = 4.2$ resonance at 10 kMHz, no $g' = 4.2$ resonance is observed at 36 kMHz.[3] Therefore, a search for a zero field absorption about 20 kMHz is planned.

2.2 Exchange Coupled Cr^{3+} Ions in Glass

In semi-annual technical report number two, it was shown that for antiferromagnetically exchange coupled Cr^{3+} ions in a phosphate glass, the ESR spectrum will be symmetrical about $g' = 2$ as long as the transition energy $h\nu$ dominates the anisotropies.[5] The ESR spectrum at 9.49 kMHz shown in that same report demonstrates that this symmetry condition is well satisfied at that frequency.[4] Further, the model used predicts that as long as the transition energy $h\nu$ dominates the anisotropies, the ESR linewidth is a constant independent of the energy of the microwave photon used. This can readily be shown with the use of the energy level diagram shown in Fig. 2. In Fig. 2, is shown the energy level diagram for an $S = 1$ system for a direction of the external magnetic field along one of the principal symmetry axes of the paramagnetic system. For external fields having arbitrary orientation relative to the magnetic axes, the effective g values and hence the absorption spectrum occurs between the values obtained along the magnetic axes. It can be seen from Fig. 2, that $\Delta M_s = \pm 1$ transitions are allowed from the $M_s = |\pm 1\rangle$ levels to $M_s = |0\rangle$ level for $h\nu > Z.F.S.$ In addition, as mentioned above these transitions are symmetrically

centered about $g' = 2.0$. The magnetic fields at which the $\Delta M_s = \pm 1$ transitions can occur are given by the relations:

$$H_1 = \frac{1}{g\beta} \; [h\nu - Z.F.S.] \text{ for } |M_s\rangle = |+1\rangle \leftrightarrow |M_s\rangle = |0\rangle \; ,$$

and

$$H_2 = \frac{1}{g\beta} \; [h\nu + Z.F.S.] \text{ for } |M_s\rangle = |-1\rangle \leftrightarrow |M_s\rangle = |0\rangle \; .$$

The resulting ESR linewidth is given by

$$\Delta H = H_2 - H_1 = \frac{2 \; Z.F.S.}{g\beta} \; , \text{ for } h\nu \rangle Z.F.S.$$

and is frequency independent. It was shown before that for exchange coupled Cr^{3+} ions in glass with a value of 60 cm^{-1} for $|J|$, the isotropic exchange coupling constant, the ESR spectrum arises predominantly from transitions within the $S = 1$ level.[5] Because of this result, it is reasonable in a qualitative analysis of the ESR spectrum for this system to consider only the transitions within the $S = 1$ level as above.

In Fig. 3 is shown the ESR spectrum of antiferromagnetically exchange coupled Cr^{3+} ions in a phosphate glass at 34.8 kMHz and at 300°K. The base glass studied has the composition 90 wt.% $Al(PO_3)_3$ and 1.3 wt.% ZnO. To this base was added 8.69 wt.% Cr_2O_3. It can be seen in Fig. 3 that the ESR spectrum is nearly isotropic about $g' = 2$ with a linewidth of 950 gauss. The ESR spectrum of this same glass at 10 kMHz shown in reference 1 is also nearly isotropic about $g' = 2$ with a linewidth of about 1000 gauss at 300°K.[1] The small differences in linewidth observed for frequencies of 9.49 and 34.8 kMHz may be due to difference in the transition probabilities at the two frequencies, to other effects of the higher S multiplets ($S = 2,3$) not considered, and to experimental errors in measurement. It is therefore concluded that the linewidth of the ESR spectrum for the exchange coupled Cr^{3+} ion pairs in glass is independent of the energy of the microwave photon used for the case $h\nu \rangle Z.F.S.$ as the model predicts. In addition, this simple model allows for an anisotropic ESR spectrum with an overall shift to higher g' - values as

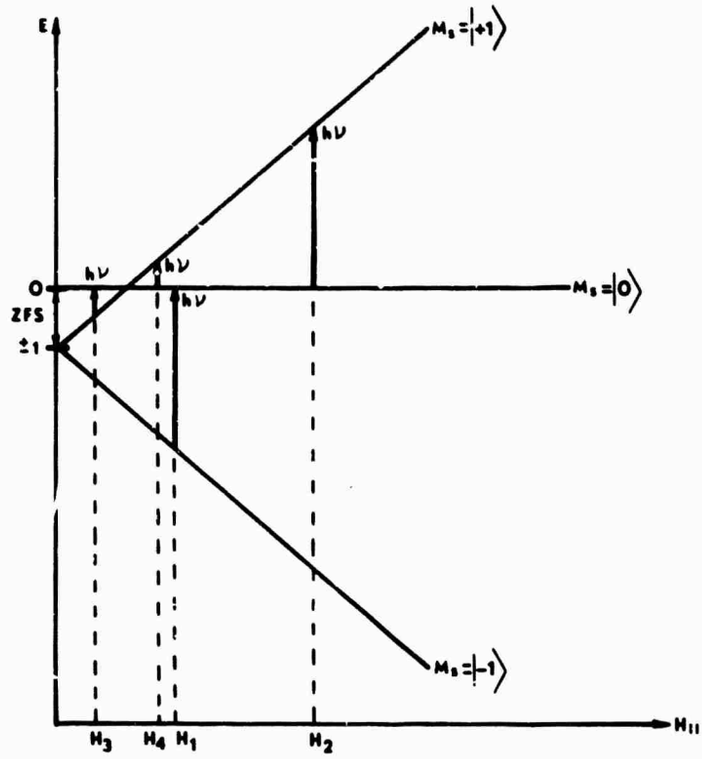

Fig. 2. Energy level diagram for S = 1 paramagnetic system for a direction of the external DC magnetic field along one of the principal magnetic axes. For $h\nu > ZFS$, transitions can occur at H_1 and at H_2. For $h\nu \sim ZFS$, transitions can occur at H_3 and H_4.

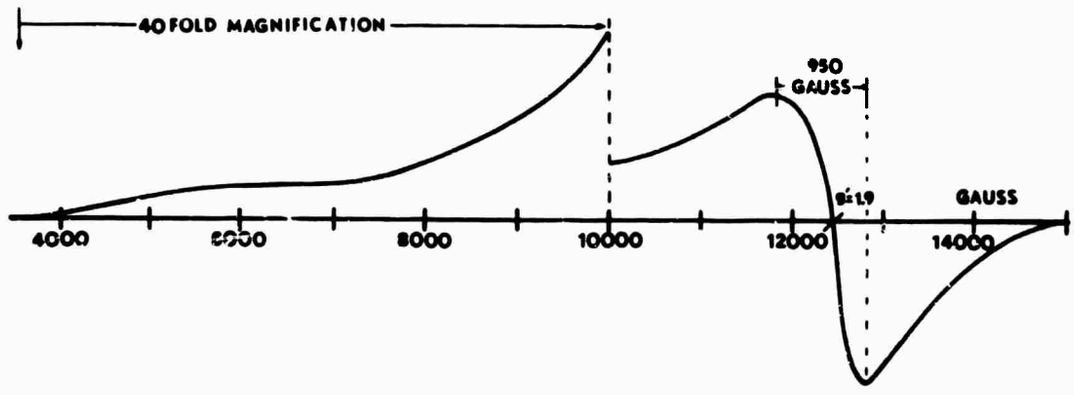

Fig. 3. ESR spectrum of antiferromagnetically exchange coupled Cr^{3+} ions in a phosphate glass at 34.8 kMHz and at 300°K.

observed in the 2.05 kMHz spectrum shown in semi-annual report number two.[5] In this latter case, where $h\nu \approx$ Z.F.S., $\Delta M = \pm 1$ transitions can be induced between the $|M_s\rangle = |0\rangle \leftrightarrow |M_s\rangle = |-1\rangle$ level shown in Fig. 2.

2.3 Isolated Cu^{2+} Ions in Silicate Glass

It was shown earlier that Cu^{2+} ions in silicate glass remain well isolated from one another below a concentration of 0.5 wt.%CuO.[4] It was further pointed out that isolated Cu^{2+} ions in silicate glass appears to be octahedrally coordinated to oxygen in a crystal field of predominantly axial symmetry.[4] The Cu^{2+} ion has an electronic magnetic spin S = 1/2, and a nuclear magnetic spin I = 3/2. In glass, the resulting hyperfine structure in the ESR powder spectrum for isolated Cu^{2+} is partially resolved for the external DC magnetic field in a direction perpendicular to the magnetic symmetry axes.[4] The magnetic parameters measured in ESR experiments are sensitively dependent on the local environment of the paramagnetic ion. Thus, a study of the dependence of the ESR magnetic parameters for Cu^{2+} ions on the glass composition can be used as a probe to study the local environment of this ion in glass. To this end a study of the magnetic $g_\perp$ and $A_\perp$ parameters, where $g_\perp$ and $A_\perp$ are the spectroscopic splitting factor and the hyperfine coupling constant for the external DC magnetic field in a direction perpendicular to the magnetic symmetry axes, as a function of the type of alkali modifier present in a simple calcium silicate glass was undertaken.

A series of calcium silicate glasses containing 0.2 mole % CuO and 20 mole % of the alkali metals Li, Na, K, Rb, and Cs were fabricated. The glasses have composition of 60 mole % SiO_2, 12 mole % CaO, 20 mole % alkali metal and 0.2 mole % CuO, All materials used are of reagent grade quality, and the compositions listed above are the starting compositions. In the first 2 columns in Table I are listed the glasses fabricated and the alkali modifier ion present. The ESR spectra at 9.49 kMHz and at 77°K of the glasses listed in Table I are shown in Fig. 4. From Fig. 4, it can be seen that the ratios of the intensities of the hyperfine lines are dependent upon the type of alkali ion present, although the dependence appears to be small.

The magnetic parameters $g_\perp$ and $A_\perp$ were calculated from the line position in magnetic field units of the hyperfine

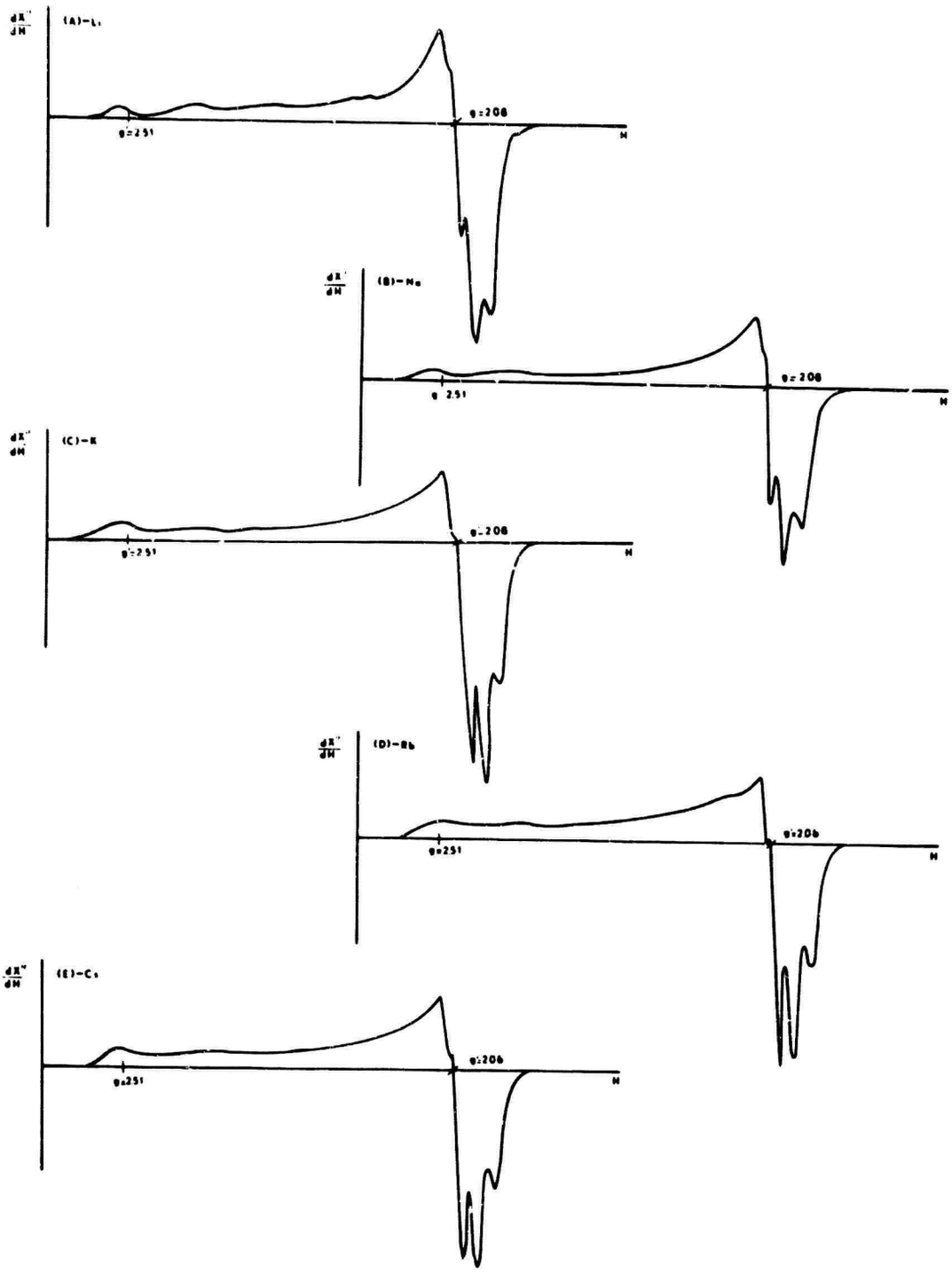

Fig. 4. ESR spectra at 9.49 kMHz and at 77°K for isolated Cu^{2+} ions in alkali-calcium silicate glass for alkali ions; (a) Li, (b) Na, (c) K, (d) Rb, and (e) Cs.

components which is given to second order by the relationship[5]

$$H(m) = \frac{h\nu_o}{\beta g_\perp} - \frac{1}{\beta g_\perp}\left\{A_\perp m - \left[\frac{A_\parallel^2 + A_\perp^2}{4h\nu_o}\right]\left[I(I+1)-m^2\right]\right\} ,$$

where m is the nuclear magnetic quantum number ($m = \pm 3/2, \pm 1/2$), and where the other symbols have the meanings defined before. Analysis of the spectra shown in Fig. 4 yields the magnetic parameters $g_\perp$ and $A_\perp$ listed in the last two columns in Table I along with the experimental error observed for repeated experiments.

Sample	Alkali Metal	$g_\perp$	$A_\perp (cm^{-1})$
A	Lithium	2.049 ± 0.001	22.4 ± 0.2x10^{-4}
B	Sodium	2.049 ± 0.001	22.5 ± 0.1x10^{-4}
C	Potassium	2.049 ± 0.001	23.8 ± 0.3x10^{-4}
D	Rubidium	2.048 ± 0.001	24.2 ± 0.1x10^{-4}
E	Cesium	2.048 ± 0.001	24.4 ± 0.2x10^{-4}

Table I. Experimental ESR parameters measured for Cu^{2+} for type of alkali modifier ion present in a calcium silicate glass. The base composition of the glass is 60 mole % SiO_2, 12 mole % CaO, 20 mole % alkali metal and 0.2 mole % CuO.

The limits of error on $g_\perp$ and $A_\perp$ above are ± .001 and ± 1x10^{-4} cm^{-1}, respectively. With this in mind it can be seen in Table I that the variations in $g_\perp$ and $A_\perp$ are very small and within the experimental limits of error. It is quite clear from the data, however, that there is no coordination number dependence of the Cu^{2+} on the type of modifier ions present. In addition, the data shows that the local environment of isolated Cu^{2+} ions in silicate glass must be such that the ESR parameters measured above are not sensitive to an approximate two-fold change in ionic radii of univalent alkali modifier ion present.[6] The presence of alkali ions may still be required, however, for charge compensating purposes.

Additional study, calculations, and analysis are required before any other definitive conclusions can be made. A limited number of additional experiments are planned.

3. EXPERIMENTAL INVESTIGATIONS OF COLOR CENTER DEFECTS IN LASER GLASS

3.1 Room Temperature Stable Color Center Defects in Laser Glass

It was shown earlier that the activation spectrum for production of room temperature stable color center defects by ultraviolet (uv) light in a laser glass has a peak at about 218 nm with a full width at half maximum of 13.0 nm.[4,5] The resulting optical absorption spectrum of the room temperature stable color centers in the wavelength region (300-1000) nm was also investigated in an earlier period.[4,5] During this period, the effects of uv irradiation on the optical absorption spectrum of the same laser glass in the wavelength region (200-300) nm was investigated. Prior to uv irradiation, the glass normally has absorptions in the range (200-300) nm as shown in Fig. 5a. In Fig. 5a and 5b is shown the optical transmission spectra in the wavelength range (200-400) nm of a 1 mm thick sample of the laser glass prior to and after uv irradiation, respectively. The composition of the glass has been given before and it is to be noted that the addition of 5 wt.% Nd_2O_3 does not appear to cause any changes in the uv induced optical absorption spectrum of the base glass throughout the range (200-1000) nm.[4,5] The spectra shown in Fig. 5 were taken on a Carey Model 14 spectrophotometer at 300°K. The optical absorption spectrum of the glass over the wavelength region (200-800) nm is shown in Fig. 6. In this figure is plotted $\log_{10} T_1/T_2$ vs. wavelength λ, where T_1 and T_2 are the transmission of the sample in the unsolarized and solarized conditions, respectively. The new feature shown in Fig. 6 is the large negative absorption which corresponds to an annihilation of absorbing centers. It can be seen from Fig. 6 that the "annihilation" spectrum has a peak at about 220 nm with a full width at half maximum of about 40 nm. It is interesting to observe that the "annihilation" spectrum above and the activation spectrum presented earlier both peak in the region of 220 nm.[5]

Additional experiments and study are required before any definitive conclusions can be reached. Further work, which includes growth and bleaching studies are planned.

3.2 Transient Color Centers

In order to properly characterize the transient color centers which give rise to limit cycle and self Q-switched laser action in glass lasers, it is of fundamental importance to determine if they can be associated with the ultraviolet induced room

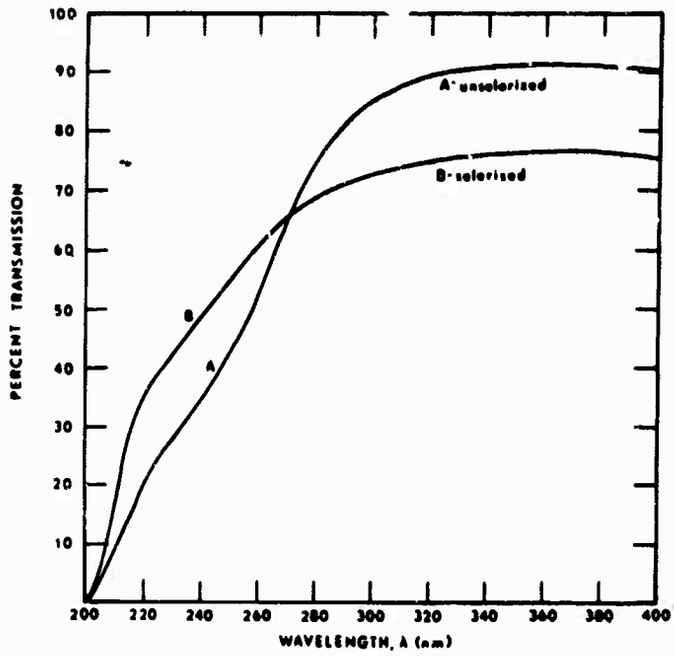

Fig. 5. Optical transmission spectra of 1 mm thick laser base glass in the wavelength region (200-400) nm in conditions: (a) unsolarized, and (b) solarized by ultraviolet light from Xenon flashtube.

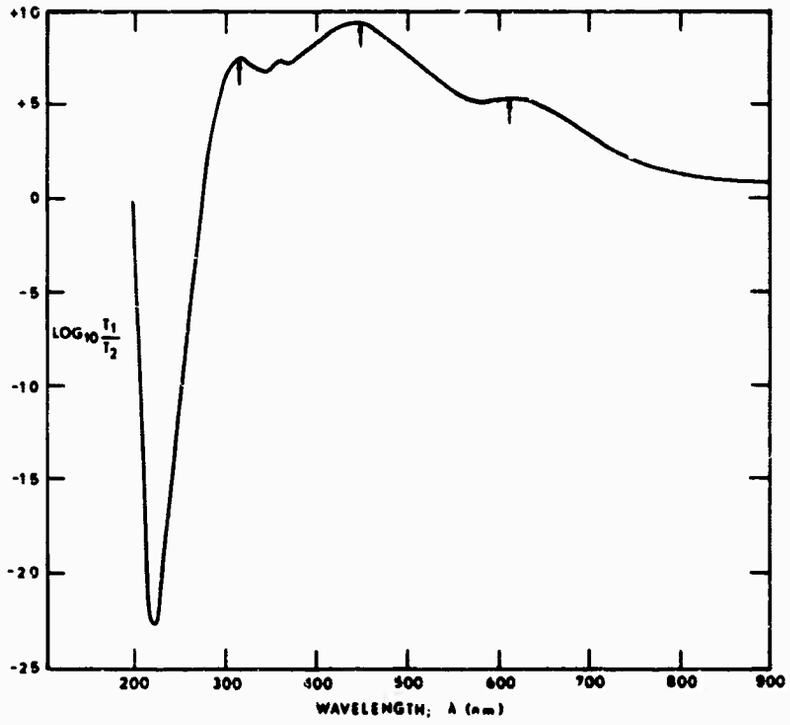

Fig. 6. Optical absorption spectrum of solarized laser base glass in the wavelength region (200-800) nm. T_1 and T_2 are the transmission of the unsolarized and solarized sample, respectively.

temperature stable color centers. Prior to this study, all experiments undertaken to determine if a relationship does exist were performed with laser glass which contained significant concentrations of Nd^{3+}.[7] The negative results of these experiments suggested that the transient centers are independent of the room temperature stable centers. Since both Nd^{3+} and the uv induced stable color centers have absorptions in the visible region of the optical spectrum, an affirmative result could be masked by the strong absorptions due to the Nd^{3+}. In semi-annual technical report number 2, it was shown that the presence of Nd^{3+} in the laser glass is not essential to the production of the transient color centers.[5] As a result of this technical development, the question of the relationship of the transient to the room temperature stable color centers was re-examined during this period. An association would be indicated in laser experiments if a growth of the self Q-switched laser output with repeated pumping in the uv could be demonstrated and/or if self Q-switched behavior could be induced by pumping into existing irradiation induced room temperature stable color center bands only in the visible portion of the optical spectrum. Preliminary experiments to determine if the transient color centers are associated with the room temperature stable color centers were undertaken during this period. The experiments performed, the results, and the conclusion derived are described below.

A diagram of an experimental laser system used is shown in Fig. 7. The laser configuration consisted of a 20 cm long, 5 mm diameter AO glass type 970 Nd^{3+} doped laser rod with 1 mm thick cladding of Kimball Glass type 'KG-12' and close wrapped with silver foil to two 12.7 cm long Xenon flashtubes. The clad laser rod had polished parallel flats on both ends. A 23 cm long, 4 mm diameter laser Q-switching clear base glass without the Nd^{3+} and with a flat at one end and a 45° roof at the other end was end coupled at the flat end to one of the flat ends of the laser rod. The mechanical coupler used fit snugly over the laser rod and the clear glass rod and contained a small hole to permit the introduction of water to fill any spaces between the flats of the laser and clear rods. It was necessary to couple the glass rods in this manner since it was found impossible to optically align this laser system because of the very poor optical quality of the clear glass rod which is highly striated. The composition of the clear Q-switching laser base glass has been given before.[4] A 65% 1.06μ dichroic was placed on the other end of the 970 laser rod as shown in Fig. 7. Hence, end reflectances of 65% was provided by the dichroic and 98% was provided by the 45° roof on the clear glass rod. The clear glass rod was pumped with an FT24A Helical Xenon flashtube connected in series with

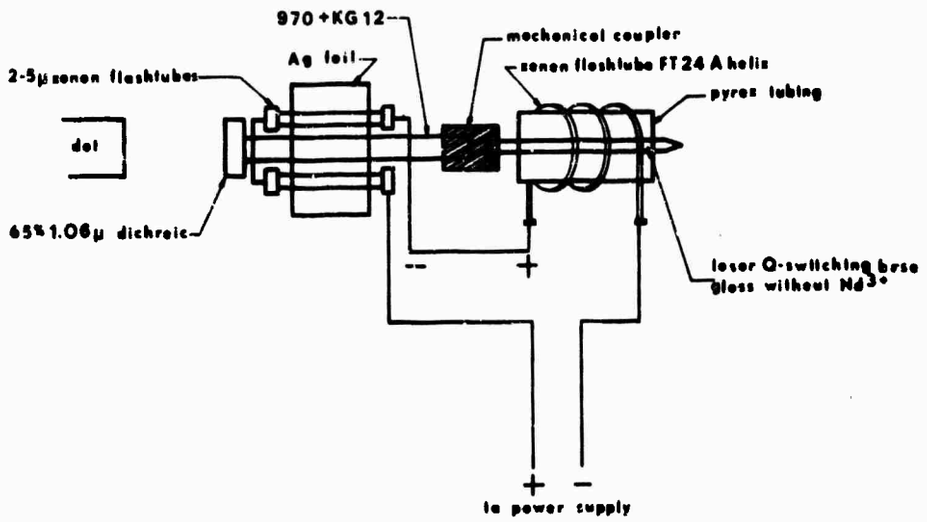

Fig. 7. Experimental laser configuration used to investigate the relationship of the transient color centers which give rise to limit cycle and self Q-switched laser action in glass lasers to the room temperature stable color centers.

the two 5U Xenon flashtubes as shown in Fig. 7. The power supply was operated at 3.5 kV with a capacitance of 280 microfarads and with an inductance of 58 microhenrys. Hence, a total of about 1700 joules was dissipated by the Xenon flashtubes. When it was desired to filter the uv from the pump light flashing the clear glass rod a cylindrical piece of Pyrex glass filter tubing of diameter 2.54 cm and 1.5 mm thickness was slid into the helical flashtube between the 4 mm diameter clear glass and the helical flashtube. Frame A in Fig. 8 shows the laser time trace obtained when the ultraviolet light is filtered from the pump light flashing the clear laser Q-switching glass base by Pyrex tubing as described above, and only when the clear glass rod is in the unsolarized condition; i.e., there are no room temperature stable color centers present. In Frame A, it can be seen that normal laser damped oscillations are obtained when pumping under these conditions. All time traces shown in Fig. 8 were taken with a sweep speed of 100 μsec/cm. Increasing time is from left to right. Time trace A was taken with a vertical sensitivity of 0.1 V/cm. Following the time trace obtained in Frame A, the Pyrex tubing was removed and five additional laser time traces were obtained with three minute time intervals between each. The laser time traces shown in Frames B and C of Fig. 8

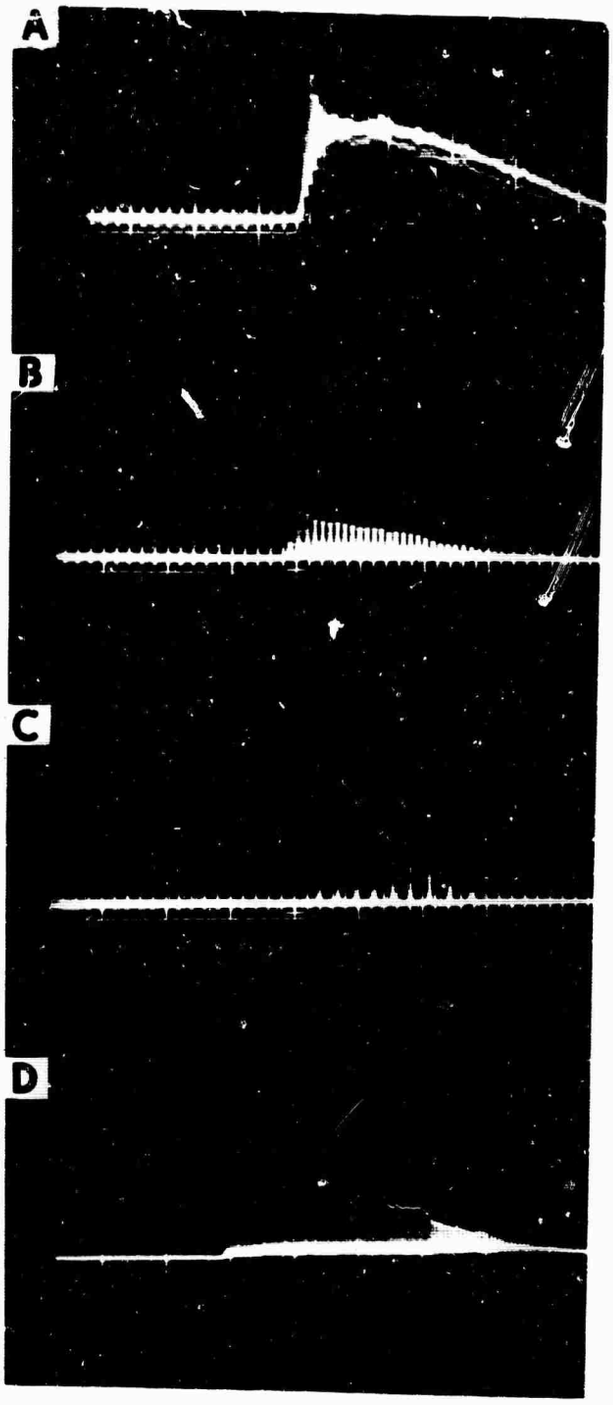

Fig. 8. Laser time traces obtained from laser system shown in Fig. 7 when the Q-switching laser base rod is: (A) not exposed to uv light and in the unsolarized condition, (B) exposed to uv light immediately following the laser trace obtained in Frame A above, (C) exposed to uv light for the fifth consecutive time, and (D) not exposed to uv light and in a solarized condition. All time traces were taken with a sweep speed of 100 μsec/cm. Frames A, B and D, and C were taken with oscilloscope vertical sensitivities of 0.1, 1, and 2 volts/cm, respectively. Increasing time is from left to right.

were the first and fifth time traces obtained, respectively. As can be seen in laser traces B and C, self Q-switched laser action is obtained when the ultraviolet light is not filtered from the pump light pumping the clear glass rod. In addition, time traces B and C were taken with a vertical sensitivity of 1V/cm and 2V/cm, respectively. In comparing these traces, it appears that the effect of the repeated exposures to the ultraviolet light is to decrease the number of Q-switched spikes in the laser Q-switching train of spikes, to increase the laser threshold, to increase the peak heights of the initial spikes, and to increase the time interval between the laser spikes. These results should only be considered in a qualitative way since the manner in which the rods were coupled might allow for significant changes in the laser output. Hence, it might be concluded that there appears to be a growth effect with repeated exposures to uv light.

Following the laser time trace shown in Frame C, the same piece of Pyrex tubing which was used in obtaining the time trace shown in Frame A was reinserted between the helical flashtube and the clear glass rod. The laser time trace shown in Frame D was subsequently obtained with an oscilloscope vertical sensitivity of 1V/cm. It can be seen from Frame D that a strong limit cycle behavior is obtained when the uv light is filtered from the light pumping the Q-switching base glass in the solarized condition. In Frame A, it was demonstrated that the Pyrex filter used does not allow for the production of the transient color centers which give rise to limit cycle and self Q-switched action in laser glass. Hence, the limit cycle behavior shown in Frame D must arise from the effects of the visible or near uv pump light from the helical flashtube on the solarized glass rod. This base glass in the solarized condition has room temperature stable optical absorption bands centered at about 310, 450, and 620 nm as shown in Section 3.1. The results shown in Frames A and D would be consistent if the transient color centers are associated with one or more of the room temperature stable absorption bands mentioned above. In addition, the growth behavior of the Q-switching effect shown in Frames B and D due to repeated exposures to uv light is to be qualitatively expected if the transient color centers are associated with the room temperature stable color centers. The preliminary results obtained thus suggest that the transient color centers which give rise to limit cycle and self Q-switched laser action in laser glass are associated with the room temperature stable color centers. This conclusion should be regarded as tentative and preliminary only. The experimental systems which suggested this conclusion are under very careful scrutiny and reexamination to insure that the results obtained are not due

entirely to some artifact of the systems used. In addition, other systems and experiments have been designed which should allow for a definitive answer to this question. Because of this development, the experimental effort to measure the lifetime of the transient color centers has been deferred until the more definitive experiments mentioned above have been concluded. However, since some time was used during this period in developing a system to measure the lifetime of the transient color center, the system developed is described below.

In a measurement of the lifetime of any transient state of a system, it is desirable to populate the transient state with a square wave excitation pulse and following the trailing edge of the pulse monitor the natural depletion time from the transient state. For an exponential depletion, the time that it takes to deplete to e^{-1} of the initial value can be taken as the natural lifetime of the transient state. With this in mind, the laser system shown in Fig. 9 was developed in order to try to measure the lifetime of the transient color centers. The salient features of the system shown in Fig. 9 include a Nd^{3+} self Q-switched glass laser rod, a clear glass rod in which the transient color centers can be induced, two power supplies, Xenon flashtubes for pumping the laser rod and for producing the transient color centers in the clear glass rod, a time delay trigger unit, a beam splitter, two detectors, and a fast rise dual beam oscilloscope. Since the transient color center has an absorption at 1.06μ, the 1.06μ light from a Nd^{3+} laser can be used as a test source. With a train of self Q-switched laser spikes, it is possible to perform absorption measurements on the first spike only. The theory of operation is in principle quite simple. As shown in Fig. 9, part of the laser light is reflected from a beam splitter to the first detector and the other part of the laser light is transmitted through the absorbing rod to the second detector. The outputs from the first and second detectors are fed to the input of a dual beam oscilloscope and the resulting display on the CRT is photographed. The intensity of the signal from the first detector serves as a reference point for the testing light which passes through the rod in which the transient color centers have been induced. From the ratio of the areas of the two signals photographed on the CRT, it is possible to determine the amount of 1.06μ light absorbed by the transient color centers.

The transient color centers can be induced by an excitation pulse from a Xenon flashtube which can be made to approximate a square wave by the use of appropriate L.C. filters and an ignitron circuit. The ignitron circuit is placed in parallel with the Xenon flashtubes. The resistance of the ignitron circuit when

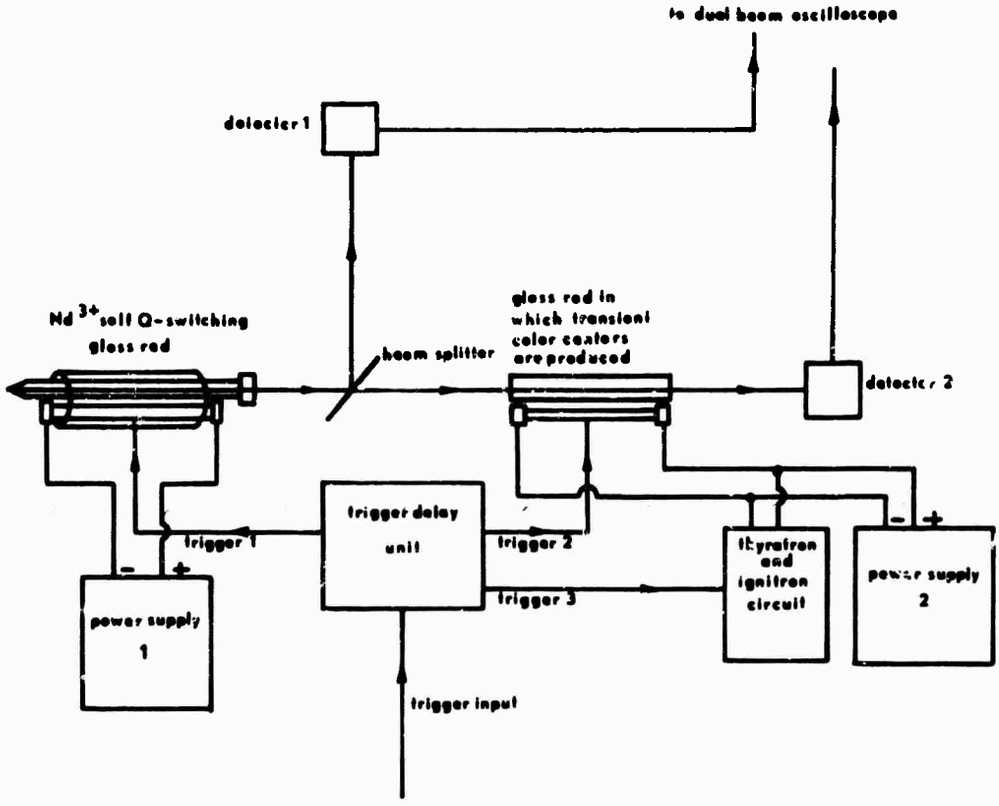

Fig. 9. Experimental laser system developed to measure the lifetime of transient color centers which give rise to limit cycle and self Q-switched laser action in laser glass.

activated (0.04 ohms) is less than that of the Xenon flashtubes in the ionized condition. Hence, when the ignitron circuit is activated while the Xenon flashtube is in the ionized condition, current flow from the power supply is diverted from the Xenon flashtube through the ignitron circuit to ground giving rise to a sharply declining trailing edge to the flashtube output. The flatness of the peak of the excitation pulse can be controlled by the choice of the inductance placed in parallel with the capacitors in the power supply. By controlling the time at which the ignitron circuit is activated following the firing of the Xenon flashtube, i.e., by controlling the delay time between triggers two and three in Fig. 9, it is possible to control the pulse width of the excitation pulse. By controlling the times at which the laser is fired and the time at which the excitation pulse is fired, i.e., by specifying the delay time between triggers one and two in Fig. 9, it is possible to make absorption measurements at any time following the trailing edge of the color center excitation pulse.

A schematic diagram of the power supply and ignitron circuit developed to give an approximately square wave excitation light pulse from a 25.4 linear Xenon flashtube is shown in Fig. 10.

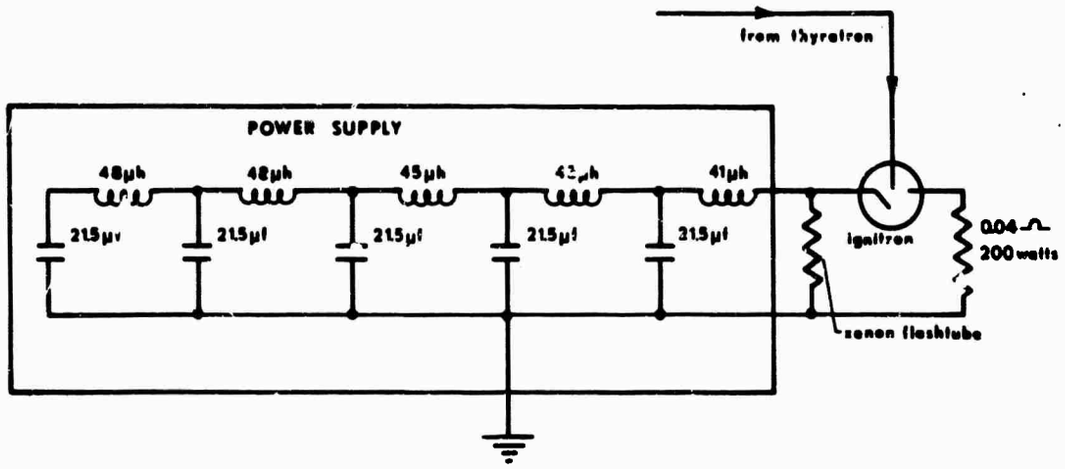

Fig. 10. Schematic diagram of power supply and ignitron circuit used for pulse shaping the light output from a 2.54 cm linear Xenon flashtube.

As can be seen in Fig. 10, an inductance of about 45 microhenrys is placed between each of the 21.5 microfarad capacitors and the load (Xenon flashtube) for purposes of pulse shaping mentioned above. The light output from the Xenon flashtube as detected by an S1 surface when the ignitron circuit is not activated is shown in Fig. 11a. The time trace shown in Fig. 11a was taken with a sweep speed of 1msec/cm. Hence, it can be seen that the 25.4 cm linear Xenon flashtube output is very nearly flat for about 2.5 millisecs with the power supply parameters shown in Fig. 10. When the ignitron circuit is activated at about 140 microsecond following the firing of the Xenon flashtube, the light output obtained from the Xenon flashtube as detected by the same S1 surface is shown in Fig. 11b. The time trace shown in Fig. 11b was taken with a sweep speed of 110 μsec/cm. Thus, it can be seen that with the use of a tuned power supply and an ignitron circuit, an approximately square wave light output from a Xenon flashtube can easily be obtained.

As mentioned earlier, lifetime measurements will be undertaken after the other more definitive experiments mentioned above to better characterize the transient color centers have been completed.

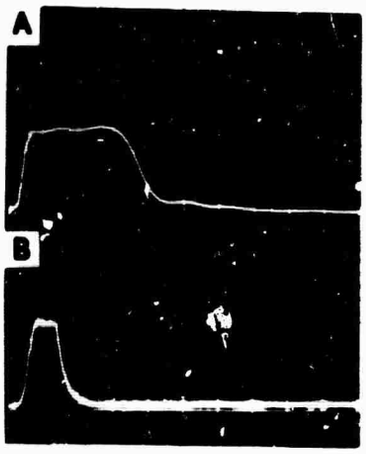

Fig. 11. Time traces of pulse shaped light output from 25.4 cm linear Xenon flashtube as detected by an S_1 surface when the ignitron circuit is: (a) not activated, and (b) activated at about 140 microseconds following the firing of the Xenon flashtube. Time traces A and B were taken with a sweep speed of 1 millisec/ and 100 μsec/cm respectively. Increasing time is from left to right.

4. COLOR CENTER CALCULATIONS

4.1 Introduction

In Semi-Annual Technical Report No. 1, a theory of the g-values of a hole trapped on a SiO_4 tetrahedron with a single non-bridging oxygen was presented.[4] In that treatment of the problem, the form of the molecular wavefunctions was determined from symmetry requirements, and qualitative arguments were used to predict the ordering of the energy levels. Expressions were obtained for the g-values which involved molecular energy differences and molecular orbital expansion coefficients. By identifying the energy differences with observed optical absorption bands, it was possible to explore the variation of the g-values with electron distribution and to make comparisons with electron spin resonance data. The results suggested that studies of tetrahedral units with more than one non-bridging oxygen should be explored in a further attempt to obtain correlations with the observed magnetic properties of the trapped hole centers. However, in considering these units one finds a multiplicity of molecular states, and direct calculation appears to provide the only basis for the prediction of the energy level scheme and the identification of optical absorptions. Consequently, the electronic structure calculations have been emphasized during this period.

The approach to the molecular calculations has been altered to take into account σ-π mixing effects. In the case of the tetrahedron with a single non-bonded oxygen, the trapped hole was found to reside either in a σ lone pair orbital of the non-bridging oxygen or in a "π" orbital constructed from oxygen 2p and Si 3d atomic orbitals. The underlying σ structure was treated separately. Precisely speaking, the mixing of the σ and π functions is demanded by symmetry. Furthermore, it appears that this mixing must be taken into account if observed hyperfine splitting are to be explained. Recent investigations of the hyperfine structure of the spin resonance spectrum of trapped hole centers in alkali silicate glasses enriched to a concentration of 68% Si^{29} indicate a Fermi contact contribution to the hyperfine splitting.[8] Since this contribution requires s-character of the trapped-hole wavefunction at the Si^{29} nucleus, a molecular orbital description in terms of d-π orbitals alone would not be adequate for determining the hyperfine structure. Consequently, it is concluded that a molecular orbital theory in which symmetry requirements are fully imposed provides a more useful approach to the structure problem.

4.2 M. O. Theory - CNDO Approximation

The method adopted for study of the SiO_4 tetrahedral units is a simplified self-consistent molecular orbital theory which has been developed and applied to a number of polyatomic molecules by Pople, Santry, and Segal.[9-12] The method is derived from the Roothaan theory,[13] but incorporates complete neglect of differential overlap (CNDO) and the emperical approximation of certain integrals. Molecular orbitals ψ_i are constructed as linear combinations of atomic valence orbitals ϕ_μ according to the prescription

$$\psi_i = \sum_\mu \phi_\mu c_{\mu i} \tag{1}$$

For a system of closed shells, minimization of the molecular energy with respect to variation of the expansion coefficients leads to the secular problem for the molecular orbitals and single electron energies

$$det\,|F_{\mu\nu} - \varepsilon S_{\mu\nu}| = 0, \tag{2}$$

where

$$F_{\mu\nu} = H_{\mu\nu} + G_{\mu\nu} ,$$

$$H_{\mu\nu} = \int \phi_\mu^* \left[-1/2\nabla^2 - \sum V_A(\vec{r}) \right] \left[\phi_\nu d\tau \right] ,$$

$$G_{\mu\nu} = \sum_{\lambda\sigma} P_{\lambda\sigma} \left[(\mu\nu|\lambda\sigma) - 1/2(\mu\sigma|\mu\lambda) \right] , \tag{3}$$

$$(\mu\nu|\lambda\sigma) = \iint \phi_\mu^*(1)\phi_\nu(1) \frac{1}{r_{12}} \phi_\mu^*(2)\phi_\sigma(2) d\tau_1 \, d\tau_2 ,$$

$$P_{\lambda\sigma} = 2 \sum_i c_{i\lambda}^* c_{i\sigma} .$$

Here, $V_A(\vec{r})$ is the potential due to the core of the Ath atomic constituent of the molecule, and the summation in the expression for $P_{\lambda\sigma}$ extends over occupied molecular orbitals. These equations are of great complexity, and without further simplification solution is limited to systems with few electrons. The approximations of the CNDO method reduce these equations to manageable form even for large molecules. Details of the development of the CNDO theory are given in References 2 through 5. Briefly the approximations are

1. $$S_{\mu\nu} = \int \phi_\mu^* \phi_\nu d\tau = \delta_{\mu\nu}$$

With this approximation the total change on center A is given by

$$P_{AA} = \sum_{\mu}^{A} P_{\mu\mu} .$$

2. All integrals involving differential overlap products $\phi_\mu \phi_\nu$ with $\mu \neq \nu$ are neglected. Thus, no exchange integrals appear. Coulomb interactions are treated approximately in that an average Coulomb integral computed for valence S-electrons is used for all valence electrons. One and two center Coulomb integrals are distinguished. For valence electrons on center A the integral γ_{AA} is defined by

$$\gamma_{AA} = (\mu\mu|\mu\mu|) ,$$

where $|\mu\rangle$ is an S atomic orbital. For valence electron on centers A and B, γ_{AB} is defined by

$$\gamma_{AB} = (\mu\mu|\nu\nu) ,$$

where $|\mu\rangle$ is an S-orbital on center A and $|\nu\rangle$ is an S orbital on center B.

3. Diagonal matrix elements $H_{\mu\mu}$ are approximated by the expression

$$H_{\mu\mu} = - 1/2 \, (I_\mu + A_\mu) - (Z_A - 1/2) \, \gamma_{AA} - \sum_{B \neq A} Z_B \, \gamma_{AB},$$

where I_μ and A_μ are the ionization potential and electron affinity of the μth electron on center A, and Z_A and Z_B are the charges on cores A and B respectively. Diagonal matrix elements of G are given by the expression

$$G_{\mu\mu} = 1/2\ P_{AA}\ \gamma_{AA} + \sum_{B\neq A} P_{BB}\ \gamma_{AB} \quad .$$

4. Off diagonal matrix elements of H are related to the overlap S through the expression

$$H_{\mu\nu} = \beta_{AB}\ S_{\mu\nu} \ ,$$

where β_{AB} is an emperically determined bonding parameter. Off diagonal elements of G reduce to

$$G_{\mu\nu} = -\ 1/2\ P_{\mu\nu}\ \gamma_{AB} \ .$$

With all these approximations taken into account, matrix elements $F_{\lambda\nu}$ are given by

$$F_{\mu\mu} = -\ 1/2\ (I_\mu + A_\mu) + \left[(P_{AA} - Z_A) - 1/2(P_{\mu\mu} - 1)\right] \gamma_{AA} + \sum_{B\neq A} (P_{BB} - Z_B)\ \gamma_{AB}$$

$$F_{\mu\nu} = \beta_{AB}\ S_{\mu\nu} - 1/2\ P_{\mu\nu}\ \gamma_{AB} \ , \quad \mu \neq \nu \quad .$$

It should be noted that valence electrons are treated equivalently in this theory. This approximation is introduced to guarantee invariance of matrix elements under coordinate and basis transformations.[9] However, in the case where d-electrons are included in the basis (as is the case for Si), a separate parameterization of the d and s,p set of functions is called for. Thus, in the case of Si, we obtain different Coulomb integrals $\gamma_{AA}(S,S)$, $\gamma_{AA}(S,D)$, $\gamma_{AA}(D,D)$ representing respectively the interaction of electrons from the s,p set, the interaction of s,p electrons with d electrons, and the interactions of d electrons. Similar generalizations apply to the two-center Coulomb integrals γ_{AB} and to the bonding parameter β_{AB}, and the expressions

for $F_{\mu\nu}$ must be altered somewhat to reflect these generalizations.[5]

4.3 Application to SiO_4 Tetrahedra

Quantum mechanical structure calculations in glass are complicated by the randomness of the network. While X-ray studies indicate that the individual tetrahedra are uniform, there is a considerable variation in the Si-O-Si bond angle at the join between adjacent tetrahedra. The approach adopted in the initial calculations undertaken here is to consider explicitly a single tetrahedron with effects of adjacent units treated superficially. For a basis atomic orbital $|\mu\rangle$ on center A, the contribution to the diagonal matrix element $F_{\mu\mu}$ due to interaction with other centers B is given by the term

$$\sum_{B \neq A} (P_{BB} - Z_B)\, \gamma_{AB} \quad .$$

In the case of an orbital associated with a non-bridging oxygen we include in the diagonal matrix element only contributions from the tetrahedron which includes the non-bridging oxygen. For an orbital belonging to a bridging oxygen, contributions from the two tetrahedra joined by that oxygen are included in the diagonal matrix element. Thus, a diagonal element for non-bridging oxygen function includes terms

$$(P(S)_{Si,Si} - Z_{Si})\, \gamma(S,S)_{Si,O} + P(D)_{Si,Si} - Z_{Si})\, \gamma(S,D)_{Si,O} + 3(P(br)_{O,O} - Z_O)\, \gamma_{O,O} \quad ,$$

while the corresponding element for a bridging-oxygen centered orbital includes terms

$$2(P(S)_{Si,Si} - Z_{Si})\, \gamma(S,S)_{Si,O} + 2\,(P(D)_{Si,Si} - Z_{Si})\, \gamma(S,D)_{Si,O} + 5(P(br)_{O,O} - Z_O)\, \gamma_{O,O}$$

$$+ (P(nbr)_{O,O} - Z_O)\, \gamma_{O,O}$$

Here br and nbr denote the charge on bridging and non-bridging oxygen respectively.

The basis set employed consists of oxygen 2s and 2p and silicon 3s, 3p, and 3d orbitals. Consequently, straightforward application of the procedure leads to a 25 x 25 secular determinant. For a specific symmetry, however, use of symmetry adapted wavefunctions reduces the size of the matrices which must be handled. For a tetrahedron with one or three non-bridging oxygen ions, the symmetry is C_{3v}, and the orbitals can be classified according to their transformation properties. With reference to Fig. 12 for the coordinate scheme used, the wavefunctions can be grouped as follows.

$$\phi(a)_{2s},\ \phi(a)_{2p^0},\ \phi(a)_{3s},\ \phi(Si)_{3p^0},\ \phi(Si)_{3d^0},\ \frac{1}{\sqrt{3}}\left(\phi(b)_{2s} + \phi(c)_{2s} + \phi(d)_{2s}\right)$$

Γ_1:

$$\frac{1}{\sqrt{3}}\left(\phi(b)_{2p^0} + \phi(c)_{2p^0} + \phi(d)_{2p^0}\right),\ \frac{1}{\sqrt{6}}\left[\left(\phi(b)_{2p^{+1}} - \phi(b)_{2p^{-1}} + \phi(c)_{2p^{+1}} - \phi(c)_{2p^{-1}}\right) + \left(\phi(d)_{2p^{+1}} - \phi(d)_{2p^{-1}}\right)\right]$$

Γ_2: $\frac{1}{\sqrt{6}}\left[\left(\phi(b)_{2p^{+1}} + \phi(b)_{2p^{-1}}\right) + \left(\phi(c)_{2p^{+1}} + \phi(c)_{2p^{-1}}\right) + \left(\phi(d)_{2p^{+1}} + \phi(d)_{2p^{-1}}\right)\right]$

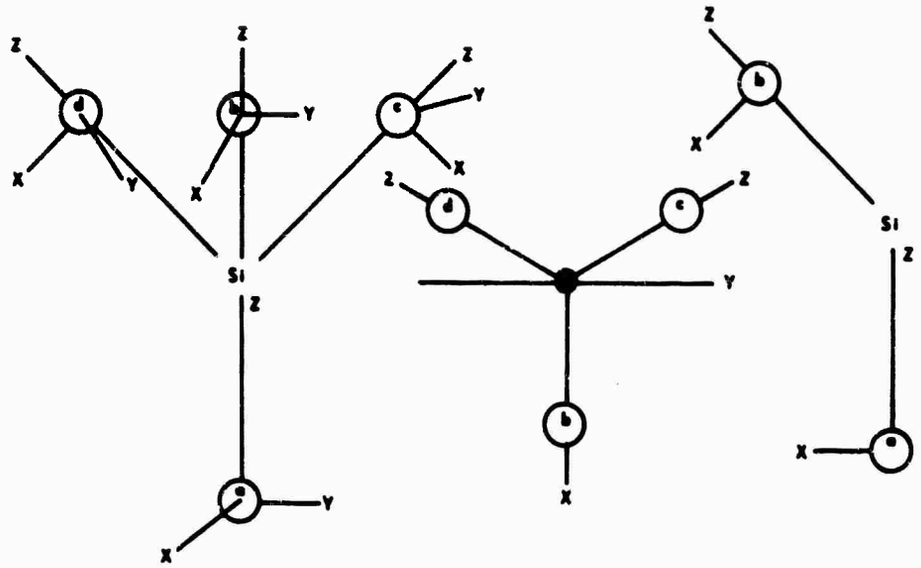

Fig. 12. Coordinates used in specifying molecular orbitals.

Γ_3: $\phi(a)_{2p^{+1}}$, $\phi(Si)_{3p^{+1}}$, $\phi(Si)_{3d^{+1}}$, $\phi(Si)_{3d^{-2}}$, $\frac{1}{\sqrt{3}}\ \phi(b)_{2s} + \omega_1\ \phi(c)_{2s} + \omega_1\ \phi(d)_{2s}$

$$\frac{1}{\sqrt{3}}\left(\phi(b)_{2p^0} + \omega_1\ \phi(c)_{2p^0} + \omega_2\ \phi(d)_{2p^0}\right),\ \frac{1}{\sqrt{3}}\left(\phi(b)_{2p^{+1}} + \omega_1\ \phi(c)_{2p^{+1}} + \omega_2\ \phi(d)_{2p^{+1}}\right),$$

Row 1:

$$\frac{1}{\sqrt{3}}\left(\phi(b)_{2p^{-1}} + \omega_1\ \phi(c)_{2p^{-1}} + \omega_2\ \phi(d)_{2p^{-1}}\right)$$

$$\phi(a)_{2p^{-1}},\ \phi(Si)_{3p^{-1}},\ \phi(Si)_{3d^{-1}}\ \phi(Si)_{3d^{+2}},\ \frac{1}{\sqrt{3}}\left(\phi(b)_{2s} + \omega_2\ \phi(c)_{2s} + \omega_1\ \phi(d)_{2s}\right)$$

Row 2: $\frac{1}{\sqrt{3}}\left(\phi(b)_{2p^0} + \omega_2\ \phi(c)_{2p^0} + \omega_1\ \phi(d)_{2p^0}\right),\ \frac{1}{\sqrt{3}}\left(\phi(b)_{2p^{+1}} + \omega_2\ \phi(c)_{2p^{+1}} + \omega_1\ \phi(d)_{2p^{+1}}\right)$

$$\frac{1}{\sqrt{3}}\left(\phi(b)_{2p^{-1}} + \omega_2\ \phi(c)_{2p^{-1}} + \omega_1\ \phi(d)_{2p^{-1}}\right)$$

$$\omega_1 = \text{EXP}\left(i\,\frac{2\pi}{3}\right) \text{ and } \omega_2 = \text{EXP}\left(-i\,\frac{2\pi}{3}\right)$$

The representations Γ_1 and Γ_2 are both one dimensional and lead to 8 x 8 and 1 x 1 secular determinants respectively. The representation Γ_3 is two dimensional and leads to two identical 8 x 8 secular problems, one for each set of eight functions transforming as a particular row of the representation. Thus, the largest secular determinant which must be solved is of dimension 8 x 8 as compared with the 25 x 25 determinant obtained for the non-symmetry adapted basis.

4.4 Evaluation of Matrix Elements

Since the CNDO method has been applied to SiH_4 and to various oxide molecules, values for most of the needed parameters are already available.[10-12] The values in Hartree atomic units of the terms 1/2(I+A) are collected in Table II.

Orbital		-1/2(I+A)(a.u.)
O:	2S	0.9331
	2P	0.3348
	3S	0.3687
Si:	3P	0.1529
	3d	0.01239

Table II. Matrix Elements for SiO_4 Calculation

Bonding parameters β_{AB} are determined using the parameterization recommended in Ref. 5; these are $\beta_{O,C}$ = - 1.1393 a.u., $\beta(S)_{Si,O}$ = - 0.6073 a.u., and $\beta(D)_{Si,O}$ = - 0.4729 a.u.

Only overlap integrals and one-and two-center Coulomb integrals are required for execution of the CNDO calculation. Slater orbitals of the form

$$\phi_{n\ell m} = N\, r^{n-1}\, e^{-kr}\, Y_\ell^m$$

are employed with exponential parameter k determined from Slater's prescription for s and p electrons.[14] The values are $k_{2s} = k_{2p} = 2.28$, $k_{3s} = k_{3p} = k_{3d} = 1.38$. In evaluating integrals for the SiO_4 tetrahedron the Si-O and O-O distances are taken to be 1.62Å and 2.65Å respectively.[17]

Evaluation of required overlap integrals is accomplished by re-expressing the orbitals involved in a coordinate system having co-linear Z axes directed along the internuclear line with the X axes chosen such that the Z axes and X axes are co-planar. Both Z axes are taken to point in the same direction. Since the atomic basis orbitals involve spherical harmonics, the transformation of the orbitals to the new coordinate systems is accomplished through application of the well known rotation matrices.[15] When this tedious procedure is undertaken, the required overlap integrals are expressed as linear combinations of elemental overlap integrals in a coordinate system with co-linear Z axes. These elemental overlap integrals can be evaluated by transformation to spheroidal coordinates.[16] A computer routine has been written to evaluate the needed integrals. Integral values are listed in Table III.

O-O	O-Si
$(2S,2S) = 0.01250$	$(2S,3S) = 0.3385$
$(2S,2p^{o}) = -0.01794$	$(2S,3p^{o}) = -0.4787$
$(2p^{o}2p^{o}) = -0.02537$	$(2S,3d^{o}) = 0.4422$
$(2p^{+1},2p^{+1}) = 0.003610$	$(2p^{o},3S^{o}) = 0.1991$
	$(2p^{o},3p^{o}) = -0.2383$
	$(2p^{o},3d^{o}) = 0.1623$
	$(2p^{+1},3p^{+1}) = 0.1798$
	$(2p^{+1},3d^{+1}) = .3000$

Table III. Elemental Overlap Integral Values

The one-center Coulomb integrals can be evaluated directly in closed form. Two-center Coulomb integrals pose a more difficult problem. The integration is facilitated by transformation to spheroidal coordinates, but a double numerical integration is required. A program for computing these integrals

has been written and successfully executed. Integral values are listed in Table IV.

One Center Integrals (a.u.)	Two Center Integrals (a.u.)
$\gamma_{O,O}(S,S) = 0.8283$	$\gamma_{O,O}(S,S) = 0.1997$
$\gamma_{Si,Si}(S,S) = 0.4532$	$\gamma_{O,Si}(S,S) = 0.3022$

Table VI. One-and two-center Coulomb Integrals for SiO_4 Calculations

4.5 Current Status

With all required integrals and matrix elements evaluated, the next step in the calculation is the incorporation of the various elements into a computational scheme for the self-consistent evaluation of the molecular orbitals and the orbital energies. A computer program for this purpose is being prepared. The execution and refinement of this program are the chief goals for the coming period.

REFERENCES

1. R.J. Landry, J.T. Fournier, and C.G. Young, J. Chem. Phys., 46, 1285 (1967).

2. L.L. van Reijan "Electron Spin Resonance Studies of Pentavalent and Trivalent Chromium," (Doctoral Thesis) Technological University at Eindhoven, 1964.

3. R. Weeks, private communication.

4. R.J. Landry, J.T. Fournier, "ESR and Optical Absorption Studies of Transition Metal Ions and Color Centers in Glass," Semi-Annual Technical Report Number one, ARPA Order No. 306, Contract No. N00014-67-C-0186, April 1967.

5. R.J. Landry, J.T. Fournier, "ESR and Optical Absorption Studies of Transition Metal Ions and Color Centers in Glass," Semi-Annual Technical Report Number two, ARPA Order No. 306, Contract No. N00014-67-C-0186, March 1968.

6. L. Pauling, The Nature of the Chemical Bond, (Cornell University Press, Ithaca, New York, 1945), p. 346.

7. W. Shiner, E. Snitzer, and R.F. Woodcock, Phys. Letters 4, 412 (1966).

8. T.A. Sidorov and V.A. Tiulkin, Akademia Nauk S.S.S.R. Doklady 175, 872 (1967) (Russ.).

9. J.A. Pople, D.P. Santry, and G.A. Segal, J. Chem. Phys. 43, 5129 (1965).

10. J.A. Pople and G.A. Segal, J. Chem. Phys. 43, 5136 (1965).

11. J.A. Pople and G.A. Segal, J. Chem. Phys. 44, 3209 (1966).

12. D.P. Santry and G.A. Segal, J. Chem. Phys. 47, 158 (1967).

13. C.C.J. Roothaan, Rev. Mod. Phys. 23, 69 (1951).

14. J.C. Slater, "Quantum Theory of Atomic Structure", Vol. 1 (McGraw-Hill Book Co. Inc., New York, 1960), p. 369.

15. M.E. Rose "Elementary Theory of Angular Momentum", (John Wiley & Sons, Inc., New York, 1963), Chap. 4.

16. A. Lofthus, Mol. Phys. (G.B.) 5, 105 (1962).

17. B. E. Warren, H. Krutter and O. Morningstar, J. Am. Ceram. Soc. 19, 202 (1936).

Unclassified

Security Classification

DOCUMENT CONTROL DATA - R&D

(Security classification of title, body of abstract and indexing annotation must be entered when the overall report is classified)

1. ORIGINATING ACTIVITY (Corporate author)	2a. REPORT SECURITY CLASSIFICATION
Central Research Laboratory American Optical Corporation Southbridge, Massachusetts	Unclassified
	2b. GROUP N/A

3. REPORT TITLE

ESR and Optical Absorption Studies of Transition Metal Ions and Color Centers in Glass

4. DESCRIPTIVE NOTES (Type of report and inclusive dates)

Semi-Annual Report No. 3, 1 October 67 - 31 March 68

5. AUTHOR(S) (Last name, first name, initial)

Landry, Robert J.
Fournier, Joseph

6. REPORT DATE	7a. TOTAL NO. OF PAGES	7b. NO. OF REFS
July 1968	31 + vii	17

8a. CONTRACT OR GRANT NO.	9a. ORIGINATOR'S REPORT NUMBER(S)
N00014-67-C-0186 b. PROJECT NO. ARPA Order No. 306 c. d.	TR-599-3 9b. OTHER REPORT NO(S) (Any other numbers that may be assigned this report)

10. AVAILABILITY/LIMITATION NOTICES

Qualified requestors may obtain copies of this report from DDC. Distribution of this document is unlimited

11. SUPPLEMENTARY NOTES	12. SPONSORING MILITARY ACTIVITY
Research is part of Project DEFENDER	Office of Naval Research Department of the Navy Washington, D.C.

13. ABSTRACT

The Electron Spin Resonance (ESR) spectrum of isolated Cr^{3+} ions at 34.8 kMHz and at 300°K is presented. Analysis of this and the spectrum obtained earlier at 9.49 kMHz serve to verify the initial estimated bounds of $0.3(|2D|(1\ cm^{-1}$ for the magnitude of the zero field splitting parameter.[1] In addition, the spectrum at 34.8 kMHz suggests that a direct zero field absorption may be obtained near 0.66 cm^{-1} or 20 kMHz. For exchange coupled Cr^{3+} ions in glass it is shown that as long as the transition energy hν dominates the anisotropies, the ESR linewidth is a constant independent of the energy of the microwave photon used. The ESR spectrum of antiferromagnetically exchange coupled Cr^{3+} ions in a phosphate glass at 34.8 kMHz is shown and compared to the spectrum at 9.49 kMHz. Both spectra have a linewidth of about 1000 gauss and demonstrate that the ESR linewidth is independent of the energy of the microwave photon used for hν)Z.F.S. The ESR spectra of isolated Cu^{2+} ions in a simple alkali-calcium-silicate glass as a function of the alkali type of modifier ion present are shown. The measured perpendicular magnetic parameters $g_\perp$ and $A_\perp$ for Cu^{2+} in these glasses are included. The variation in the magnetic parameters mentioned above as a function of the type of alkali modifier ion present is small and within the limits of error in measurement. The data indicates no coordination number change and shows that the local environment of the Cu^{2+} ion must be such that the ESR parameters are not very sensitive to an approximate two-fold change in ionic radii of univalent alkali modifier ion present. The effect of ultraviolet (uv) irradiation on the optical absorption spectrum of a laser glass in the wavelength region (200-300) nm is shown. It is demonstrated that the effect of uv irradiation is to cause the glass to become more transparent in the wavelength region (200-280)nm. The "annihilation" spectrum thus observed has a peak at about 220 nm, nearly coincident with the peak of the activation spectrum presented earlier,[6] and has a full width at half maximum of about 40 nm. The irradiation induced optical absorption spectrum of this same laser glass over the wavelength region (200-800) nm is shown. An experimental study to determine if the transient color centers which give rise to limit cycle and self Q-switched laser action in glass lasers are related to the room temperature stable color centers is described. The results obtained suggest that the transient color centers are associated with the stable room temperature color centers. A laser system designed to measure the lifetime of the transient color centers is described.

DD FORM 1 JAN 64 1473

Unclassified

Security Classification

14. KEY WORDS	LINK A		LINK B		LINK C	
	ROLE	WT	ROLE	WT	ROLE	WT
Glass Glass Structure Laser Glass Lasers ESR Measurements Color Centers						

INSTRUCTIONS

1. ORIGINATING ACTIVITY: Enter the name and address of the contractor, subcontractor, grantee, Department of Defense activity or other organization *(corporate author)* issuing the report.

2a. REPORT SECURITY CLASSIFICATION: Enter the overall security classification of the report. Indicate whether "Restricted Data" is included. Marking is to be in accordance with appropriate security regulations.

2b. GROUP: Automatic downgrading is specified in DoD Directive 5200.10 and Armed Forces Industrial Manual. Enter the group number. Also, when applicable, show that optional markings have been used for Group 3 and Group 4 as authorized.

3. REPORT TITLE: Enter the complete report title in all capital letters. Titles in all cases should be unclassified. If a meaningful title cannot be selected without classification, show title classification in all capitals in parenthesis immediately following the title.

4. DESCRIPTIVE NOTES: If appropriate, enter the type of report, e.g., interim, progress, summary, annual, or final. Give the inclusive dates when a specific reporting period is covered.

5. AUTHOR(S): Enter the name(s) of author(s) as shown on or in the report. Enter last name, first name, middle initial. If military, show rank and branch of service. The name of the principal author is an absolute minimum requirement.

6. REPORT DATE: Enter the date of the report as day, month, year; or month, year. If more than one date appears on the report, use date of publication.

7a. TOTAL NUMBER OF PAGES: The total page count should follow normal pagination procedures, i.e., enter the number of pages containing information.

7b. NUMBER OF REFERENCES: Enter the total number of references cited in the report.

8a. CONTRACT OR GRANT NUMBER: If appropriate, enter the applicable number of the contract or grant under which the report was written.

8b, 8c, & 8d. PROJECT NUMBER: Enter the appropriate military department identification, such as project number, subproject number, system numbers, task number, etc.

9a. ORIGINATOR'S REPORT NUMBER(S): Enter the official report number by which the document will be identified and controlled by the originating activity. This number must be unique to this report.

9b. OTHER REPORT NUMBER(S): If the report has been assigned any other report numbers *(either by the originator or by the sponsor)*, also enter this number(s).

10. AVAILABILITY/LIMITATION NOTICES: Enter any limitations on further dissemination of the report, other than those imposed by security classification, using standard statements such as:

(1) "Qualified requesters may obtain copies of this report from DDC."

(2) "Foreign announcement and dissemination of this report by DDC is not authorized."

(3) "U. S. Government agencies may obtain copies of this report directly from DDC. Other qualified DDC users shall request through

_____."

(4) "U. S. military agencies may obtain copies of this report directly from DDC. Other qualified users shall request through

_____."

(5) "All distribution of this report is controlled. Qualified DDC users shall request through

_____."

If the report has been furnished to the Office of Technical Services, Department of Commerce, for sale to the public, indicate this fact and enter the price, if known.

11. SUPPLEMENTARY NOTES: Use for additional explanatory notes.

12. SPONSORING MILITARY ACTIVITY: Enter the name of the departmental project office or laboratory sponsoring *(paying for)* the research and development. Include address.

13. ABSTRACT: Enter an abstract giving a brief and factual summary of the document indicative of the report, even though it may also appear elsewhere in the body of the technical report. If additional space is required, a continuation sheet shall be attached.

It is highly desirable that the abstract of classified reports be unclassified. Each paragraph of the abstract shall end with an indication of the military security classification of the information in the paragraph, represented as *(TS), (S), (C), or (U)*.

There is no limitation on the length of the abstract. However, the suggested length is from 150 to 225 words.

14. KEY WORDS: Key words are technically meaningful terms or short phrases that characterize a report and may be used as index entries for cataloging the report. Key words must be selected so that no security classification is required. Identifiers, such as equipment model designation, trade name, military project code name, geographic location, may be used as key words but will be followed by an indication of technical context. The assignment of links, roles, and weights is optional.